

# Fractal Structure of the Harper Map Phase Diagram from Topological Classification

Pedro Castelo Ferreira

Department of Physics, University of Oxford, 1 Keble Road, Oxford, OX1 3NP, UK  
e-mail: pcastelo@thphys.ox.ac.uk

It is suggested a *topological* hierarchical classification of the infinite many Localized phases figuring in the phase diagram of the Harper map for anisotropy parameter  $\epsilon$  versus Energy. The magnetic flux is taken to be the irrational golden mean,  $\omega^* = (\sqrt{5} - 1)/2$ . This system is equivalent to the semiclassical problem of Bloch electrons in a uniform magnetic field (Azbel-Hofstadter model). A rule that explain the fractal structure of the phase diagram is proposed. [OUTP-00-08S]

Pacs: 03.65.Sq, 05.45.+b, 71.23.Ans Keywords: Harper, Azbel-Hofstadter, Phase Transition, Fractal

This article follows [1]. The main new idea is the *topological* classification of the several Localized phases. Although the physical meaning is not completely understood, the fractal structure of the phase diagram emerge naturally in this framework.

The Schrödinger equation for the Azbel-Hofstadter model [2,3] of Bloch electrons in a uniform magnetic field can be reduced, in the Landau gauge, to the Harper equation [4]

$$\psi_{n+1} + \psi_{n-1} + 2\epsilon \cos(2\pi(\phi_0 + \omega n))\psi_n = E\psi_n \quad (1)$$

where  $\psi_n$  is the discretized wave function,  $\epsilon$  is the ratio between the  $x$  and  $y$  spacing of the underlying periodic potential and  $\omega$  is the magnetic flux over one unit cell. Under the transformation of variables  $x_n = \psi_{n-1}/\psi_n$  we obtain the Harper map [5]

$$x_{n+1} = \frac{-1}{x_n - E + 2\epsilon \cos(2\pi\phi_n)} \quad (2)$$

where  $\phi_n = (\phi_0 + \omega n) \bmod 1$ . We restricted  $\phi$  to the interval  $[0, 1]$  with identification  $0 \cong 1$ . Since it is just a phase this restriction and periodic identification cannot affect the physical results.

The Lyapunov exponent corresponding to the  $\phi$  dynamics is 0 and the one concerning the  $x$  dynamics is given by

$$\lambda = \lim_{N \rightarrow \infty} \frac{1}{N} \sum_{n=0}^N y_n \quad (3)$$

where  $y_n = \log \frac{\partial x_{n+1}}{\partial x_n} = \log x_{n+1}^2$

Aubry and André [6] proved that the Lyapunov exponent  $\lambda = -2\gamma$ , being  $\gamma$  the localization length. For the Harper map  $\lambda \leq 0$ . For  $\lambda = 0$ , the phase is Extended (E) and for  $\lambda < 0$  the phase is Localized (L).

The  $\epsilon \times E$  phase diagram of the Harper map (2) is obtained numerically and a classification, valid for irrational values of  $\omega$  is proposed. Although this classification is not valid for rational values of  $\omega$  some information about the fractal structure can be obtained from

the phase diagrams for rational values which are approximants of the irrational one.

The rational succession  $\omega_m = F_{m-1}/F_m$  converges to the irrational golden mean  $\omega^* = (\sqrt{5} - 1)/2$ . Being  $F_0 = F_1 = 1$  and  $F_m = F_{m-1} + F_{m-2}$  the  $m$ th Fibonacci number. Considering successive elements of this succession is possible to *visualize* the fractal structure of the irrational  $\omega^*$  emerging in the phase diagrams. Concerning the purpose of this work it is enough to describe the behavior of the map in the localized phases. For some  $\omega_m$ , the map has 0-dimensional attractors with period  $F_m$ , this means that the attractor is a  $F_m$ -cycle. In the limit  $\omega \rightarrow \omega^*$  it becomes an unidimensional attractor, that is a line. These results are present in figure 1.

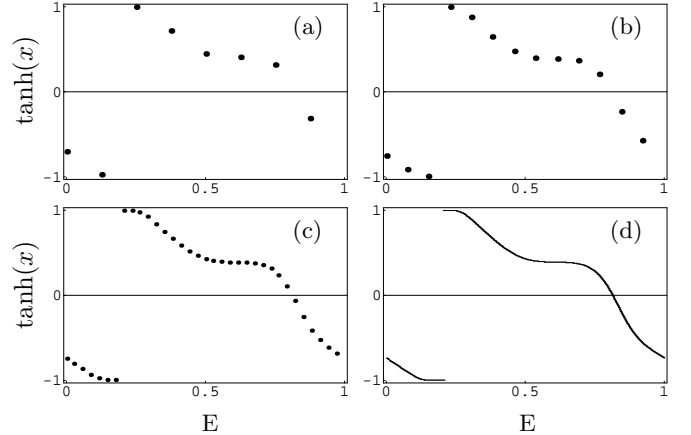


FIG. 1. Attractors corresponding to the biggest L phase for  $\phi_0 = 0$ ,  $E = 0.75$  and  $\epsilon = 0.5$ . (a)  $\omega = 5/8$ ; (b)  $\omega = 8/13$ ; (c)  $\omega = 89/144$ ; (d)  $\omega = \omega^*$ , in this limit the  $F_m$ -cycle becomes a line.

Moving through successive approximants of  $\omega^*$  the E phases split and new thinner L phases emerge. Their number increases until it become infinite. More precisely for some  $\omega_m$  there are  $F_{m-1}$  L phases in the first quadrant. Two of such diagrams are pictured in figure 2 for  $\omega = 5/8$  and  $\omega = 8/13$ . Note that the diagram is symmetric with respect to both axes  $E = 0$  and  $\epsilon = 0$ , for this reason only the first quadrant is presented.

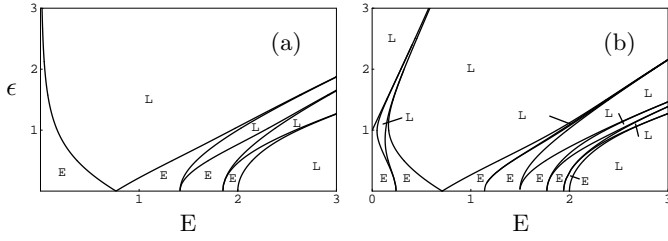


FIG. 2. Phase diagram for rational  $\omega$  for  $\phi_0 = 0$ . The Localized phases (L) are presented. (a)  $\omega = 5/8$ ; (b)  $\omega = 8/13$ .

The phase transition lines become denser and denser and they eventually cross at the critical value  $\epsilon = 1$ . The Lyapunov exponents go to zero at these points of intersection which become the ends of the lines. The phase diagram becomes in the limit of irrational  $\omega^*$  a fractal (see figure 3 and 4), more exactly, a Cantor set [7].

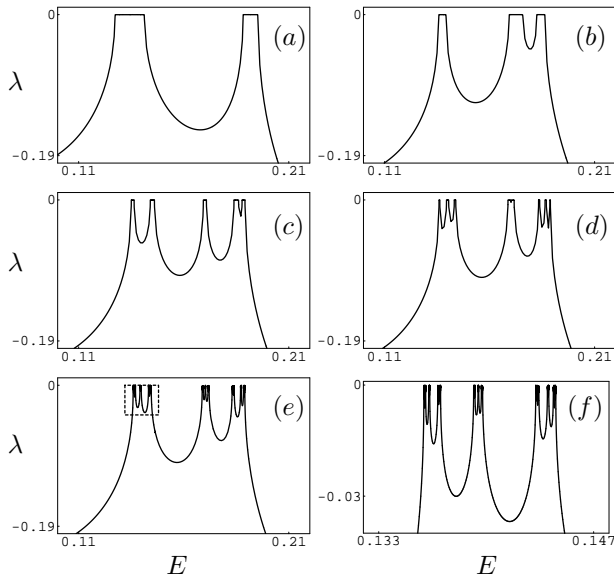


FIG. 3. Fractalization of the phase diagram. Lyapunov exponents  $\lambda$  for  $\epsilon = 1$  and  $\phi_0 = 0$ . (a)  $\omega = 13/21$ ; (b)  $\omega = 21/34$ ; (c)  $\omega = 34/55$ ; (d)  $\omega = 55/89$ ; (e)  $\omega^*$ ; (f)  $\omega^*$ , zoom of (e).

Note that for  $\epsilon > 1$  the Lyapunov exponents become always negative. This means that the phase transitions are smooth without undergoing an E phase. See [1] for further details.

It is time to define the classification. Take a map from the space  $x \times \phi$  to a torus such that the identifications  $0 \cong 1$  for  $\phi$  and  $+\infty \cong -\infty$  for  $x$  are imposed. The  $\phi$  identification is justified straight forwardly and have already been discussed. The  $x$  identification is somehow more subtle. The  $\phi \times x$  diagram is giving us local physical properties of the wave function. But at the same time we completely loose all the information about the spatial localization (and ordering) of where (and in which order) the wave function have those properties.

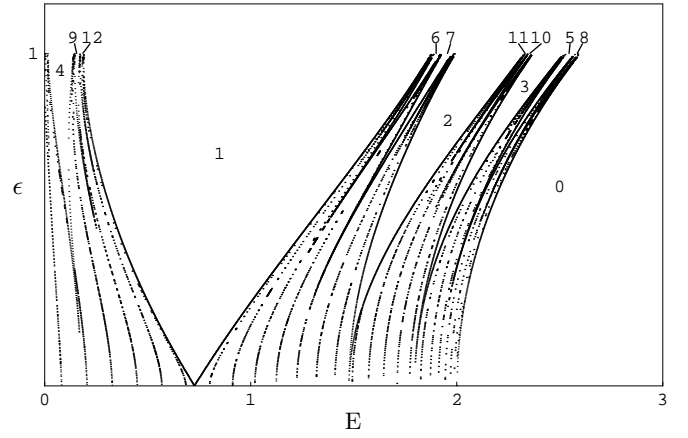


FIG. 4. Phase diagram for  $\omega^*$ . The first 12 zones are labeled in the diagram.

Further, the  $x$  variable is describing exactly the same physics when it is  $+\infty$  and  $-\infty$ . The particular property referred here is the wave function having a 0 at some (or many infinite) points since,  $x_n = \psi_{n-1}/\psi_n = \infty$ , means that  $\psi_n = 0$ . Formalizing this statement consider figure 5 where two such points, at different spatial localizations, are taken into account. The discretized points  $\psi_{n-1}$ ,  $\psi_n$ ,  $\psi_{n'-1}$  and  $\psi_{n'}$  are represented in the picture. Take in both cases  $|\psi_{n-1}| \gg |\psi_n|$  and  $|\psi_{n'-1}| \gg |\psi_{n'}|$ . This means that  $x_n \sim +\infty$  and  $x_{n'} \sim -\infty$ . Both kind of situations will always occur for irrational  $\omega$  (many times for large  $N$ ) by the simple fact that the period of the wave and the period of the underlying discretized lattice are *incompatible*.

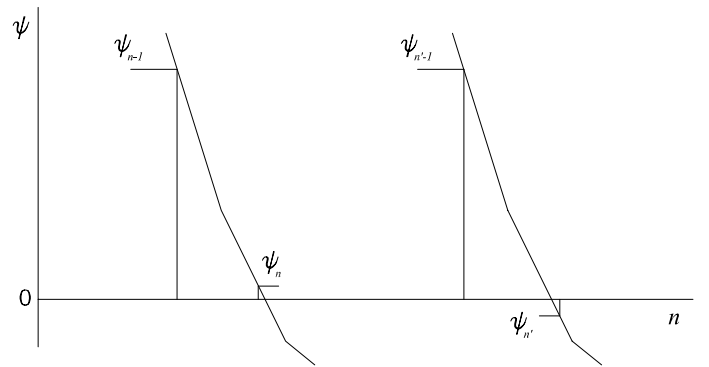


FIG. 5. The wave function is null,  $\psi = 0$ , at two distinct spatial points but the corresponding  $x$  have opposite signs.

Now the unidimensional attractors, for irrational  $\omega^*$ , are close contours living on the surface of a torus. Take as label of the classification  $\eta$ , the winding number of the line attractors along the homology corresponding to the  $x$  axis. Note that the winding number in  $\phi$  direction is always 1 except for  $E = 0$  and  $\epsilon < 1$  where there are two lines with winding number 0 in the  $x$  axis and 1 in the  $\phi$  axis [8]. It is not included in this classification.

The great advantage of the hierarchy and labels of this classification is that it coincides with the ordering of the areas occupied by the corresponding Localized phases. The diagram for irrational  $\omega^*$  and the classification of areas up to  $\eta = 12$  is presented in figure 4. The attractors for  $\eta = 10$  and  $\eta = 11$  are presented in figure 6 as an example.

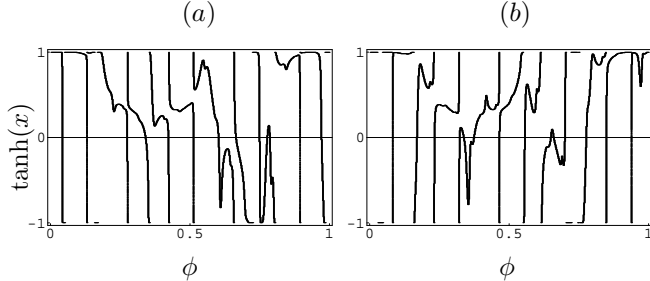


FIG. 6. Maps for  $\omega^*$  and  $\epsilon = 1$ . (a)  $\eta = 11$ ,  $E = 2.342$ ; (b)  $\eta = 10$ ,  $E = 2.347$ .

Let us define the generic rules to build the fractal structure of the first quadrant.

First remember that for each approximant  $\omega_m$  there are  $F_{m-1}$  Localized phases such that from  $\omega_m$  to  $\omega_{m+1}$  emerge exactly  $F_{m-2}$  new phases. It seems then a good guess to organize the phases in layers such that in each layer there are  $F_m$  of them. A triangular structure is formed in this way.

By inspection, in each new diagram for successive approximants the last phase on the far right (for  $E > 2$ ) has always  $\eta = 0$ . This label is not going to be taken in account, it is always present and doesn't contribute anything to explain the structure. The last new phase on the far right (just before  $\eta = 0$ ) to emerge at each approximant corresponds always to one label belonging to the Fibonacci succession  $\eta = F_{m'}$  for some  $m' \leq m$ . So, in our triangle, the last label in the right at each level

$m'$  is given by  $F_{m'}$  (see figure 7). In every level there are exactly  $F_{m'-2}$  labels such that  $F_{m'-1} < \eta_{\text{level } m'} \leq F_{m'}$ .

Proceeding to distribute the remaining labels in each level, consider the triangle completely built up to level  $k$  and let us construct the next level  $k + 1$ . Call the first element in the bottom right vertex (at level  $k$ )  $\eta_k^* = F_k$ . Now group the labels on the edges of the triangle already built in pairs starting from  $\eta_k^*$  and excluding any eventual element of level  $k$  lying in the left edge, this means  $(\eta_k^*, \eta_{k-1}^*), (\eta_{k-2}^*, \eta_{k-3}^*), \dots$ . The elements of the first pair  $(\eta_k^*, \eta_{k-1}^*)$  are summed together to give the label  $\eta_{k+1}^* = F_{k+1}$  which is placed in the right edge of the next level. We take then  $\eta_k^*$  and sum it to the elements of the remaining pairs  $(\eta_{k-2}^*, \eta_{k-3}^*), (\eta_{k-4}^*, \eta_{k-5}^*), \dots$ . The resulting elements  $(\eta_k^* + \eta_{k-1}^*, \eta_k^* + \eta_{k-2}^*), \dots$  will be placed in the new level  $k + 1$  between the original pair that was used to generate them. If up to that level there are no labels in a lower level between the original pair we swap them, otherwise they are placed after the left (before the right) original generators and before (after) other eventual labels that exist in between the original generators. It is important the spatial relation, it corresponds directly to the localization of the phases in the phase diagram. Note that in this way we are always generating new pairs of labels in the bulk of the triangle. After finishing the pairs in the edges we proceed to sum  $\eta_k^*$  to the remaining bulk pairs of level  $k' < k$  only and applying the same previous rules. Note that the bulk pairs at level  $k$  will be only used to generate new pairs for level  $k'' > k + 1$ . It is remaining one final check, from 3 in 3 levels will happen (due to the structure of the Fibonacci succession-even, odd, odd) that we cannot group the labels in the edges in pairs because their are in odd number. In that case we take the last element in the left edge (bottom) which have been left alone (it will be  $\eta = F_{k-3} + F_{k-5}$ ) and sum to it  $\eta_k^*$  placing it at the left edge of the level  $k + 1$  we are finishing to build.

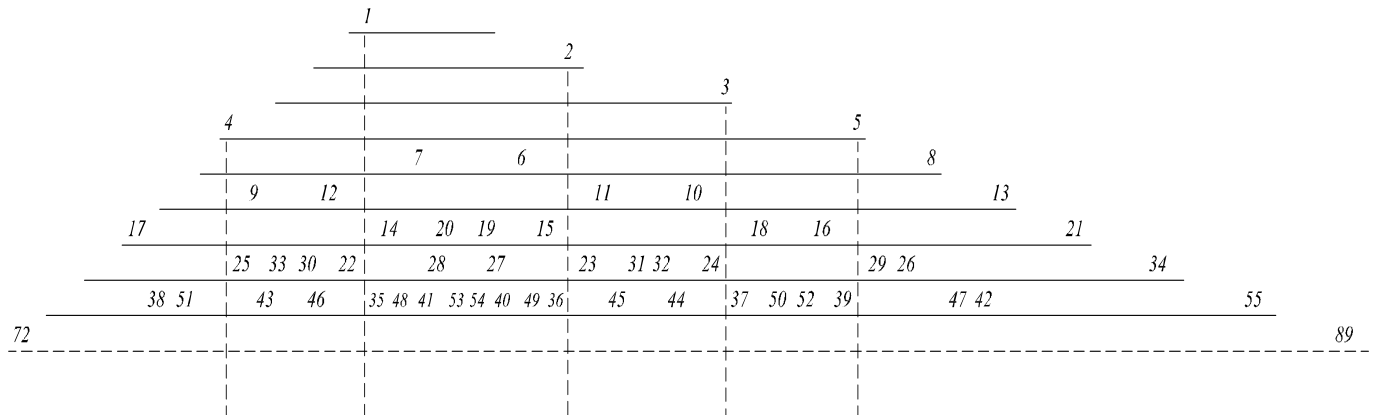


FIG. 7. Fractal structure of the phase diagram. Compare with the diagram of figure 4.

In this way the rules defining the triangular structure are complete!

The first nine levels of the triangle are shown in figure 7. On the top of the triangular structure is placed  $\eta = 1$ . The  $\eta_{m'}^* = F_{m'}$  are distributed, in sequence, on the right edge of the triangle. On the left edge the  $m'$  levels are filled only for  $m' = 3m'' + 1$  (for every  $m''$ ) with labels  $\eta = F_{3m''} + F_{3m''-2}$ . Compare figure 7 with the corresponding phases in the diagram (figure 4).

In this paper have been proposed an integer topological classification for the infinite many Localized phases of the harper map, or equivalently of the Azbel-Hofstadter problem, with an irrational magnetic flux  $\omega^* = (\sqrt{5} - 1)/2$ . It is based in the holonomy cycles of the line attractors in the  $\phi \times x$  space. Based in that classification the fractal structure of the  $E \times \epsilon$  phase diagram is built and organized into a triangular structure. It exactly describes the phase diagram taking account of the ordering of the several phases. Moreover the classification labels (1, 2, 3, ...) are exactly corresponding to the phase importance,

concerning their area or order of appearance in the succession.

This work is supported by PRAXIS XXI/BD/11461/97 grant from FCT (Portugal). The author would like to thank Francesco P. Mancini and Marcelo Tragtenberg useful discussions and comments in the manuscript which allowed to clarify some questions.

- 
- [1] P. Castelo Ferreira, F. P. Mancini and M. H. R. Tragtenberg, cond-mat/0011239
  - [2] M. Ya Azbel, Sov. Phys. JETP **19**,634 (1964).
  - [3] D. R. Hofstadter, Phys. Rev. **B14**, 2239 (1976).
  - [4] P. G. Harper, Proc. Phys. Soc. London **A68**, 874 (1955).
  - [5] J. A. Ketoja and I. I. Satija, Physica **D109**, 70 (1997).
  - [6] S. Aubry and G. André, Ann. Israel Phys. Soc. **3**, 133 (1980).
  - [7] J. Bellissard and B. Simon, J. Funct. Anal. **48**, 408 (1982).
  - [8] A. Prasad, R. Ramaswamy, I. I. Satija and N. Shah, Phys. Rev. Lett. **83**, 4530 (1999).